Corrections

PHARMACOLOGY

Correction for "Selective activation of the M_1 muscarinic acetylcholine receptor achieved by allosteric potentiation," by Lei Ma, Matthew Seager, Marion Wittmann, Marlene Jacobson, Denise Bickel, Maryann Burno, Keith Jones, Valerie Kuzmick Graufelds, Guangping Xu, Michelle Pearson, Alexander McCampbell, Renee Gaspar, Paul Shughrue, Andrew Danziger, Christopher Regan, Rose Flick, Danette Pascarella, Susan Garson, Scott Doran, Constantine Kreatsoulas, Lone Veng, Craig W. Lindsley, William Shipe, Scott Kuduk, Cyrille Sur, Gene Kinney, Guy R. Seabrook, and William J. Ray, which appeared in issue 37, September 15, 2009, of *Proc Natl Acad Sci USA* (106:15950–15955; first published August 26, 2009; 10.1073/pnas.0900903106).

The authors note that the author name Matthew Seager should have appeared as Matthew A. Seager. The online version has been corrected. The corrected author line and related footnotes appear below.

Lei Ma[1], Matthew A. Seager[1], Marion Wittmann[1], Marlene Jacobson, Denise Bickel, Maryann Burno, Keith Jones, Valerie Kuzmick Graufelds, Guangping Xu, Michelle Pearson, Alexander McCampbell, Renee Gaspar, Paul Shughrue, Andrew Danziger, Christopher Regan, Rose Flick, Danette Pascarella, Susan Garson, Scott Doran, Constantine Kreatsoulas, Lone Veng, Craig W. Lindsley, William Shipe, Scott Kuduk, Cyrille Sur, Gene Kinney, Guy R. Seabrook, and William J. Ray

Author contributions: L.M., M.A.S., M.W., M.J., A.M., P.S., C.R., S.D., C.K., C.S., G.K., and W.J.R. designed research; L.M., M.A.S., M.W., D.B., M.B., K.J., V.K.G., G.X., M.P., A.M., R.G., A.D., R.F., D.P., S.G., C.K., L.V., and W.S. performed research; M.J., C.W.L., W.S., and S.K. contributed new reagents/analytic tools; L.M., M.A.S., M.W., M.J., A.M., P.S., C.R., S.D., C.K., L.V., C.W.L., S.K., C.S., G.K., G.R.S., and W.J.R. analyzed data; and W.J.R. wrote the paper.

[1]L.M., M.A.S., and M.W. contributed equally to this work.

www.pnas.org/cgi/doi/10.1073/pnas.0910597106

ANTHROPOLOGY

Correction for "Additional evidence on the use of personal ornaments in the Middle Paleolithic of North Africa," by Francesco d'Errico, Marian Vanhaeren, Nick Barton, Abdeljalil Bouzouggar, Henk Mienis, Daniel Richter, Jean-Jacques Hublin, Shannon P. McPherron, and Pierre Lozouet, which appeared in issue 38, September 22, 2009, of *Proc Natl Acad Sci USA* (106:16051–16056; first published August 28, 2009; 10.1073/pnas.0903532106).

The authors note that Abdeljalil Bouzouggar should be credited for designing and performing the research. The corrected author contributions footnote appears below.

Author contributions: F.d., M.V., N.B., and A.B. designed research; F.d., M.V., N.B., A.B., H.M., D.R., J.-J.H., S.P.M., and P.L. performed research; F.d., M.V., and H.M. analyzed data; and F.d., M.V., N.B., and S.P.M. wrote the paper.

www.pnas.org/cgi/doi/10.1073/pnas.0910440106

PERSPECTIVE

Correction for "Feeding aquaculture in an era of finite resources," by Rosamond L. Naylor, Ronald W. Hardy, Dominique P. Bureau, Alice Chiu, Matthew Elliott, Anthony P. Farrell, Ian Forster, Delbert M. Gatlin, Rebecca J. Goldburg, Katheline Hua, and Peter D. Nichols, which appeared in issue 36, September 8, 2009, of *Proc Natl Acad Sci USA* (106:15103–15110; first published September 8, 2009; 10.1073/pnas.0905235106).

The authors note that an additional institutional affiliation should be listed for author Ian Forster: Oceanic Institute, 41-202 Kalanianaole Highway, Waimanalo, HI 96795. The corrected author line, affiliation line, and a related footnote appear below.

Rosamond L. Naylor[a,1], Ronald W. Hardy[b], Dominique P. Bureau[c], Alice Chiu[a], Matthew Elliott[d], Anthony P. Farrell[e], Ian Forster[e,f], Delbert M. Gatlin[g,h], Rebecca J. Goldburg[i], Katheline Hua[c], and Peter D. Nichols[j]

[a]Program on Food Security and the Environment, Stanford University, Encina East 404, Stanford, CA 94035; [b]Hagerman Fish Experiment Station, University of Idaho, 3059F Nat Fish Hatchery Road, Hagerman, ID 83332; [c]Department of Animal and Poultry Science, University of Guelph, Guelph, ON, Canada N1G 2W1; [d]Sea Change Management, 423 Washington Street, Third Floor, San Francisco, CA 94111; [e]Center for Aquaculture and Environmental Research, 4160 Marine Drive, West Vancouver, BC, Canada V7V 1N6; [f]Oceanic Institute, 41-202 Kalanianaole Highway, Waimanalo, HI 96795; [g]Department of Wildlife and Fisheries Sciences and Intercollegiate Faculty of Nutrition, Texas A&M University, College Station, TX 77843-2258; [h]Aquaculture Protein Centre, Norwegian Center of Excellence, N-1432 Ås, Norway; [i]Pew Environment Group, Pew Charitable Trusts, 901 E Street, 10th Floor, Washington, DC 20004; and [j]Food Futures Flagship, Marine and Atmospheric Research, Commonwealth Scientific and Industrial Research Organization, Castray Esplanade, Hobart TAS 7000, Australia

[1]To whom correspondence should be addressed. E-mail: roz@stanford.edu.

www.pnas.org/cgi/doi/10.1073/pnas.0910577106

APPLIED PHYSICAL SCIENCES

Correction for "High-sensitivity microfluidic calorimeters for biological and chemical applications," by Wonhee Lee, Warren Fon, Blake W. Axelrod, and Michael L. Roukes, which appeared in issue 36, September 8, 2009, of *Proc Natl Acad Sci USA* (106:15225–15230; first published August 24, 2009; 10.1073/pnas.0901447106).

The authors note that, due to a printer's error, on page 15227, right column, the equation on lines 14 and 15 of the first full paragraph appeared incorrectly. This error does not affect the conclusions of the article. The corrected equation appears below.

$$E = \int_0^{t_m} GV(t)/S \; dt$$

www.pnas.org/cgi/doi/10.1073/pnas.0910433106

Selective activation of the M_1 muscarinic acetylcholine receptor achieved by allosteric potentiation

Lei Ma[a,1], Matthew A. Seager[a,1], Marion Wittmann[a,1], Marlene Jacobson[b], Denise Bickel[a], Maryann Burno[a], Keith Jones[a], Valerie Kuzmick Graufelds[a], Guangping Xu[a], Michelle Pearson[a], Alexander McCampbell[a], Renee Gaspar[c], Paul Shughrue[c], Andrew Danziger[c], Christopher Regan[c], Rose Flick[b], Danette Pascarella[b], Susan Garson[d], Scott Doran[d], Constantine Kreatsoulas[e], Lone Veng[c], Craig W. Lindsley[e], William Shipe[e], Scott Kuduk[e], Cyrille Sur[f], Gene Kinney[c], Guy R. Seabrook[a], and William J. Ray[a,2]

[a]Alzheimer's Research, [c]Integrative Systems Neuroscience, [d]Depression and Circadian Disorders, [e]Medicinal Chemistry, [b]Schizophrenia Research, and [f]Imaging Merck Research Laboratories, West Point, PA 19486

Edited by Robert J. Lefkowitz, Duke University Medical Center, Durham, NC, and approved July 22, 2009 (received for review February 17, 2009)

The forebrain cholinergic system promotes higher brain function in part by signaling through the M_1 muscarinic acetylcholine receptor (mAChR). During Alzheimer's disease (AD), these cholinergic neurons degenerate, therefore selectively activating M_1 receptors could improve cognitive function in these patients while avoiding unwanted peripheral responses associated with non-selective muscarinic agonists. We describe here benzyl quinolone carboxylic acid (BQCA), a highly selective allosteric potentiator of the M_1 mAChR. BQCA reduces the concentration of ACh required to activate M_1 up to 129-fold with an inflection point value of 845 nM. No potentiation, agonism, or antagonism activity on other mAChRs is observed up to 100 μM. Furthermore studies in $M_1^{-/-}$ mice demonstrates that BQCA requires M_1 to promote inositol phosphate turnover in primary neurons and to increase c-fos and arc RNA expression and ERK phosphorylation in the brain. Radioligand-binding assays, molecular modeling, and site-directed mutagenesis experiments indicate that BQCA acts at an allosteric site involving residues Y179 and W400. BQCA reverses scopolamine-induced memory deficits in contextual fear conditioning, increases blood flow to the cerebral cortex, and increases wakefulness while reducing delta sleep. In contrast to M_1 allosteric agonists, which do not improve memory in scopolamine-challenged mice in contextual fear conditioning, BQCA induces β-arrestin recruitment to M_1, suggesting a role for this signal transduction mechanism in the cholinergic modulation of memory. In summary, BQCA exploits an allosteric potentiation mechanism to provide selectivity for the M_1 receptor and represents a promising therapeutic strategy for cognitive disorders.

Basal forebrain cholinergic neurons innervate information processing centers in the hippocampus and cortex to promote attention and memory. During AD, these neurons profoundly degenerate, contributing to cognitive impairment (1). While cholinesterase inhibitors demonstrate the therapeutic potential for boosting cholinergic function in AD, they are limited by tolerability and provide modest benefit, thus there remains a tremendous need for improved therapies (2). Selectively targeting the ACh receptors involved in memory, while sparing receptors involved in other physiological processes, could provide additional efficacy, a widely pursued approach that has yet to lead to new medicines.

ACh signals by activating ligand-gated ion channels (nicotinic receptors) and metabotropic (muscarinic) G protein-coupled receptors (GPCRs) designated M_1–M_5. Among the mAChRs, M_1 is most abundantly expressed in the hippocampus, cortex, and striatum, and localizes to postsynaptic membranes (3), where it signals via G_q/G_{11} G-proteins to phospholipase C and through other G-proteins to additional signaling systems (4, 5). M_1 regulates several ion channels including KCNQ inwardly rectifying K^+ currents, voltage-gated calcium channels, and NMDA receptors (4–9). Thus M_1 could mediate much of the cognitive effects of ACh. Supporting this hypothesis xanomeline, an M_1/M_4 preferring agonist, improved cognition and behavior in AD patients but was not tolerated due to unwanted cholinergic effects (10). Additional studies suggest that M_1 activation could slow AD progression by reducing Aβ42 peptides (11). Thus a drug that activates M_1 could potentially improve cognition while over time slowing the progression of the disease. Unfortunately, conservation of the ACh binding site has precluded the discovery of selective agonists.

Many GPCRs, including mAChRs (12), have allosteric binding sites bound by small molecules that activate the receptor in the absence of ligand (allosteric agonist) or enhance the response to native ligand (positive allosteric modulator) (13). As allosteric sites are theoretically under less evolutionary constraint, targeting them affords opportunities for selectivity. This concept was demonstrated by the M_1 allosteric agonist TBPB (14) and a collection of relatively selective positive allosteric modulators (15). Here we describe BQCA [1-(4-methoxybenzyl)-4-oxo-1,4-dihydroquinoline-3-carboxylic acid], an orally available drug-like molecule that regulates memory and brain function by potentiating M_1.

Results

Identification of BQCA. To identify M_1 potentiators a screen was conducted on >1,000,000 compounds (see *Materials and Methods*). CHO cells stably expressing human M_1 and an NFAT-responsive β-lactamase reporter to monitor Gq activation were treated with the EC_{15} of acetylcholine (15 nM) plus 6.23 μM of test compound. Compounds that increased signal more than 3 standard deviations from the mean, but had no effect in the absence of ACh, were selected for confirmation. This strategy yielded BQCA (Fig. 1*A*), which is unrelated to other muscarinic ligands. BQCA alone had no effect on calcium mobilization up to 10 μM but increased ACh potency 128.8 ± 20.1-fold at 100 μM (n = 12) (Fig. 1*B*), with an inflection point (IP) value when potentiating 3 nM ACh of 845 ± 27 nM (n = 225) (Fig. 1*C*). Similar potentiation was observed in CHO cells stably expressing rhesus, dog, rat, or mouse M_1 [IP = 300 ± 30 (n = 25), 300 ± 23 (n = 20), 330 ± 24 (n = 26), 210 ± 11(n = 32), respectively]. At 100 μM BQCA activated M_1 in the absence of ACh to an approximate 50% maximal response (Fig. 1*C*). BQCA was then tested up to 100 μM on the other human mAChRs. For M_2 and M_4, CHO cells stably expressed the mutant

Author contributions: L.M., M.A.S., M.W., M.J., A.M., P.S., C.R., S.D., C.K., C.S., G.K., and W.J.R. designed research; L.M., M.A.S., M.W., D.B., M.B., K.J., V.K.G., G.X., M.P., A.M., R.G., A.D., R.F., D.P., S.G., C.K., L.V., and W.S. performed research; M.J., C.W.L., W.S., and S.K. contributed new reagents/analytic tools; L.M., M.A.S., M.W., M.J., A.M., P.S., C.R., S.D., C.K., L.V., C.W.L., S.K., C.S., G.K., G.R.S., and W.J.R. analyzed data; and W.J.R. wrote the paper

Conflict of interest statement: All authors were employed by Merck and Company, Inc. at the time of this study

This article is a PNAS Direct Submission.

Freely available online through the PNAS open access option.

[1]L.M., M.A.S., and M.W. contributed equally to this work.

[2]To whom correspondence should be addressed. E-mail: james_ray@merck.com.

This article contains supporting information online at www.pnas.org/cgi/content/full/0900903106/DCSupplemental.

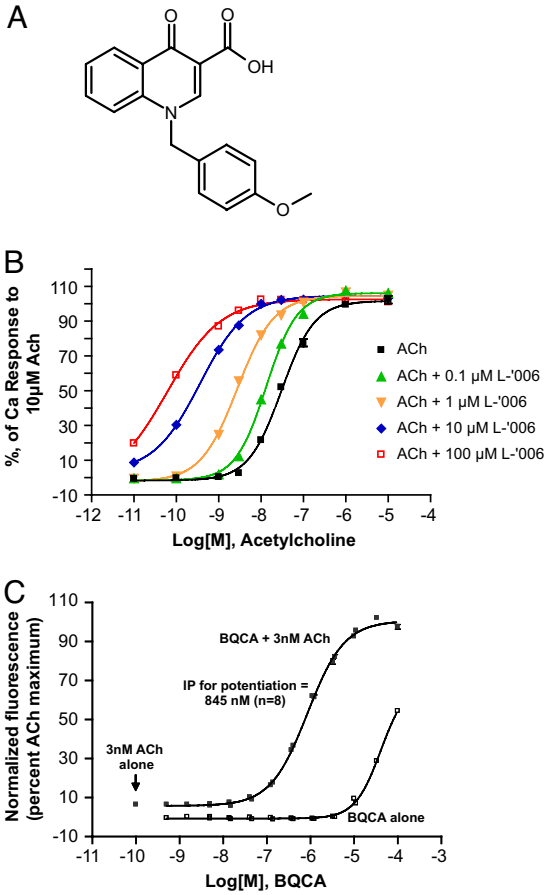

Fig. 1. Potentiation Activity of BQCA. (*A*) Structure of BQCA. (*B*) Calcium mobilization measured by FLIPR in hM_1-CHO cells induced by ACh (black line), or in the presence of BQCA at the indicated concentrations (colored lines). BQCA does not change the maximal response but causes a leftward shift in the ACh dose-response curve. Mean values from four replicate wells are plotted; data are representative of 12 independent experiments. (*C*) BQCA effects on calcium mobilization in hM_1-CHO cells as measured by FLIPR when added at the indicated concentrations alone (bottom line) or in the presence of 3 nM ACh (top line). Effect of 3 nM ACh alone is plotted as single point, lower left corner. Each point is the mean of eight replicate determinations ± SEM and is representative of 225 independent experiments.

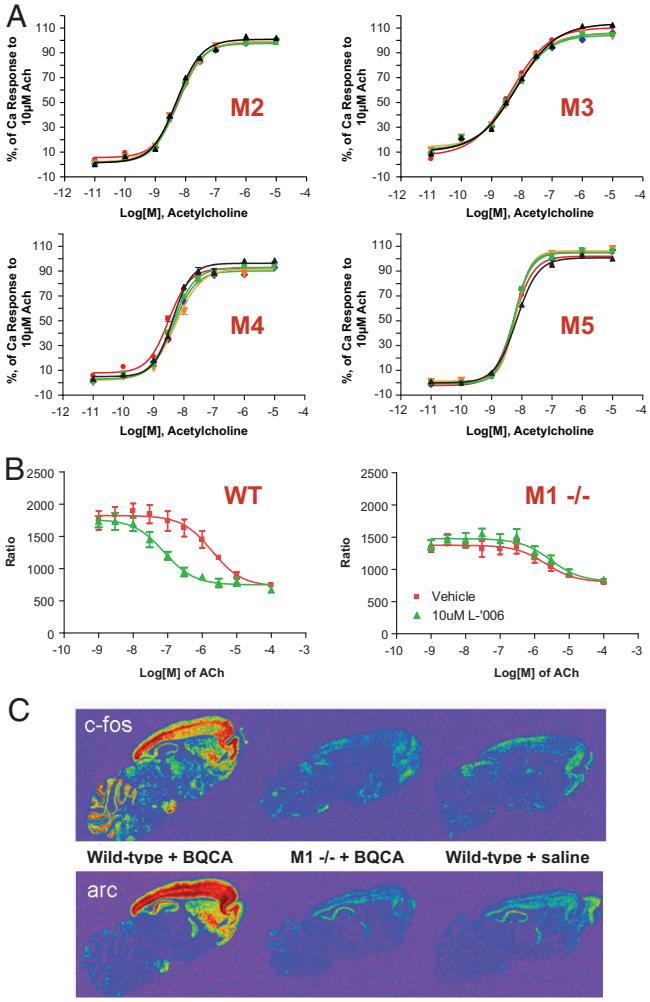

Fig. 2. Selectivity of BQCA. (*A*) BQCA effects on calcium mobilization measured by FLIPR on M_2-M_5 mAChRs in CHO cells; legend as in Fig. 1*B*. Mean values from four replicate wells are plotted. To measure calcium mobilization by M_2 and M_4, which are Gi coupled and do not normally elicit a calcium response, a permissive recombinant G protein, Gqi5, was expressed in those cell lines. BQCA had no effect on the other human mAChRs at the highest concentrations tested (100 μM). Data shown are representative of >3 independent measurements. (*B*) IP1 measurements by HTRF in wild-type or $M_1^{-/-}$ mouse primary neurons shows that ACh causes a dose-dependent decrease in counts, indicating increased IP1 levels and thus inositol phosphate metabolism, in wild-type and $M_1^{-/-}$ neurons. Error bars, SEM. (n = four replicate wells) and the data are representative of four independent experiments. (*C*) In situ hybridization for c-Fos (*Top*) and arc (*Bottom*) RNAs in sagital sections of wild-type or $M_1^{-/-}$ mice brains taken 1.5 h after oral dosing with 15 mg/kg BQCA or vehicle (saline).

G protein Gqi5 (16), which allows these Gi-coupled receptors to activate phospholipase C, permitting direct comparison between receptor subtypes. No effect was detected on M_2–M_5, indicating >100-fold selectivity (Fig. 2*A*). To rule out the possibility that selectivity was caused by differences in M_1 expression, [3H]-NMS binding to membrane preparations was measured and revealed that levels were comparable (see *Materials and Methods*). Next we addressed the possibility that selectivity over M_2 and M_4 was due to the artificial G protein. BQCA had no effect on [^{35}S]-GTPγS binding, which measures the recruitment of activated G-proteins, in CHO cells expressing M_2 or M_4 and only endogenous G-proteins (Fig. S1). BQCA had no activity in >300 radioligand binding and enzyme assays at 10 μM (see *Materials and Methods*) and did not significantly potentiate eight other class A GPCRs at 37.5 μM (Fig. S2). BQCA is a low molecular weight (331.3 Da) quinolone carboxylic acid that when dosed orally at 10 mg/kg in rats achieves brain concentrations approximating its potency (Fig. S3). Thus BQCA is a drug-like molecule that potentiates M_1 with >100-fold selectivity.

Selectivity on Native Receptors. ACh increases inositol triphosphate (IP3) metabolism in neurons by activating endogenous M_1, M_3, or M_5 receptors. To determine if BQCA is selective over endogenous neuronal mAChRs, primary mouse cortical neurons were treated with vehicle or BQCA (10 μM) for 10 min then ACh for 30 min, and levels of the IP3 metabolite IP1 were measured by homogeneous time resolved fluorescence (HTRF). As expected ACh increased IP1 as evidenced by reduction in HTRF signal; this effect was potentiated 23.3 ± 3.0-fold (n = 4) by 10 μM BQCA (Fig. 2*B*). When cultures from $M_1^{-/-}$ mice were analyzed, ACh increased IP1 levels but BQCA showed no effect, confirming selectivity for M_1.

Selectivity in Vivo. To evaluate the effects of BQCA on c-fos and arc RNA induction, markers of neuronal activation, mice were treated orally with 15 mg/kg BQCA and brains were collected 90 min later

PHARMACOLOGY

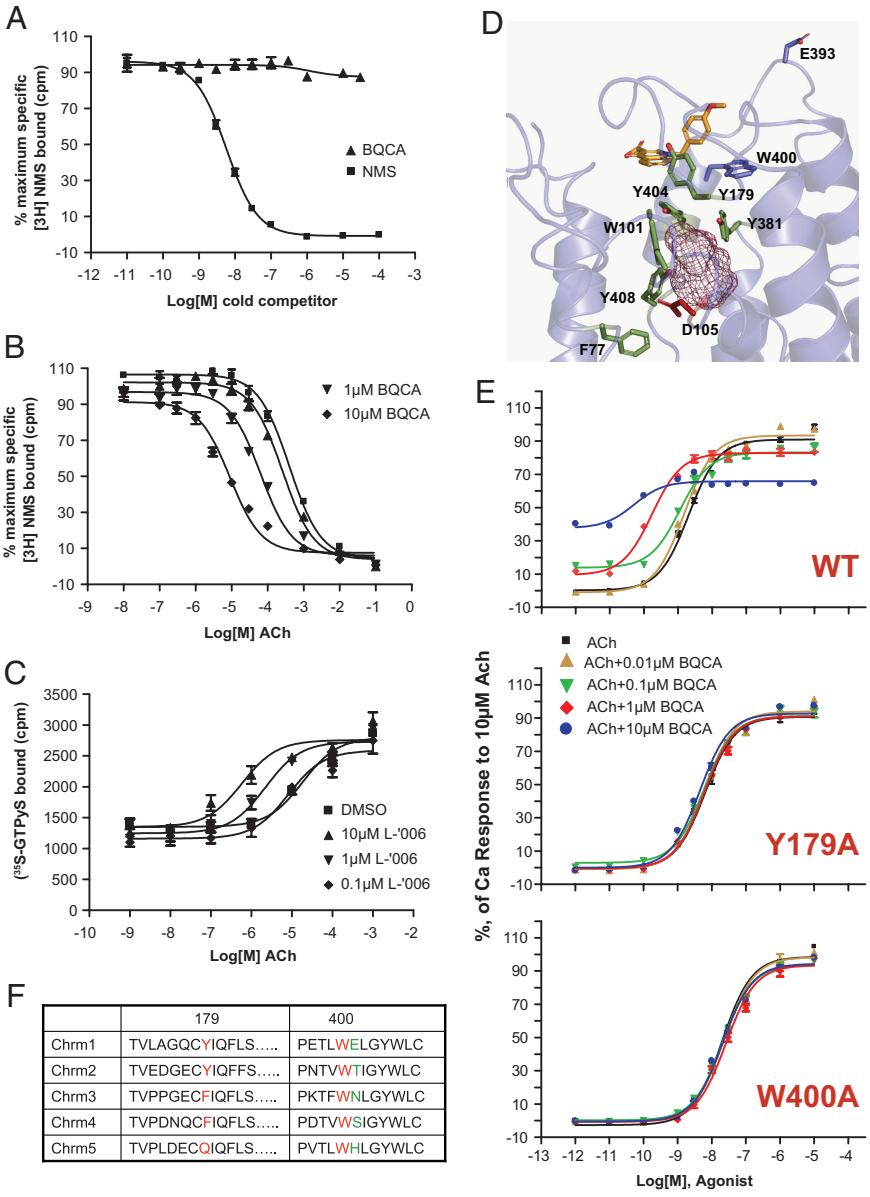

F

	179	400
Chrm1	TVLAGQCYIQFLS.....	PETLWELGYWLC
Chrm2	TVEDGECYIQFFS.....	PNTVWTIGYWLC
Chrm3	TVPPGECFIQFLS.....	PKTFWNLGYWLC
Chrm4	TVPDNQCFIQFLS.....	PDTVWSIGYWLC
Chrm5	TVPLDECQIQFLS.....	PVTLWHLGYWLC

Fig. 3. BQCA is an allosteric potentiator. (*A*) Radioligand displacement assay using hM_1-CHO membranes with unlabeled NMS (circles) and BQCA (triangles). Error bars, SEM ($n = 4$ replicate wells) and the data are representative of three experiments. (*B*) Radioligand binding assay measuring the displacement of NMS from hM_1-CHO membranes by ACh ± BQCA. (*C*) [^{35}]S-GTPγS bound to hM_1-CHO membranes in the presence of ACh (squares) or increasing concentrations of BQCA. Error bars, SEM (n = four replicate wells); data are representative of three experiments. (*D*) Molecular modeling of the M_1 extracellular region proximal to the ACh (red space-filling diagram in the center) binding site. A potential BQCA binding site was identified near amino acids Y179 and W400. (*E*) FLIPR data from Y179A and W400A mutations for ACh (black line) plus BQCA (colored lines). Legend and data format is as in Fig. 1*B*. (*F*) Amino acids flanking Y179 and W400 in human mAChRs.

for in situ hybridization. In wild-type mice, BQCA induced c-fos and arc RNA in the cortex, hippocampus, and cerebellum; arc was also elevated in the striatum (Fig. 2*C*). In contrast BQCA had no effect in $M_1^{-/-}$ mice. We then assessed the phosphorylation of ERK in wild-type and $M_1^{-/-}$ mouse cortex and hippocampus. ERK phosphorylation is a common downstream signaling event that functions in synaptic plasticity and memory (17). In wild-type mice, 15 mg/kg BQCA dosed orally increased the ratio of phosphoERK (pERK) to total ERK as revealed by western blot (28% increase, $n = 6$, $P = 0.007$, one-way ANOVA, Fig. S4). There was no effect on total ERK levels or cortical pERK. The increase in pERK was absent in $M_1^{-/-}$ mice.

Mechanism of Potentiation. We next determined if BQCA interacted with the ACh binding site. In radioligand competition assays 100 μM BQCA had no effect on the binding of the ACh-site directed antagonist [^{3}H]-N-methyl-scopolamine (NMS) to hM_1-CHO membranes (Fig. 3*A*). Instead BQCA reduced the concentration of ACh required to displace [^{3}H]-NMS 45-fold at 10 μM (Fig. 3*B*), and enhanced [^{35}S]-GTPγS binding to hM_1-CHO membranes in response to ACh 32-fold at 10 μM (Fig. 3*C*). Using Schild analysis, BQCA decreased the concentration of ACh required to displace [3H]-NMS across all concentrations tested, but did not change the dose ratio, indicating that it does not exhibit cooperativity with ACh under equilibrium binding conditions (Fig. S5). Therefore BQCA binds an allosteric site to enhance the binding and efficacy of ACh.

Interaction with the Extracellular Domain. Molecular modeling was used to dock BQCA into human M_1. A potential extracellular binding site was identified near ACh close to residues Y179, which is in the loop between transmembrane domains IV and V, and W400, which precedes transmembrane domain VII (Fig. 3*D*). We mutated Y179 and W400 to alanine; both mutations abrogated the effect of BQCA without affecting ACh (Fig. 3*E*). These two residues and their immediately adjacent amino acids are 100% conserved in rhesus, dog, rat, and mouse M_1. In contrast Y179 is not well conserved in other human mAChRs, and although whereas W400 is, E401 is not conserved and only M_1 possesses a negatively charged residue at this position (Fig. 3*F*). Thus sequence diversity in the regions near Y179 and W400 could underlie BQCA selectivity.

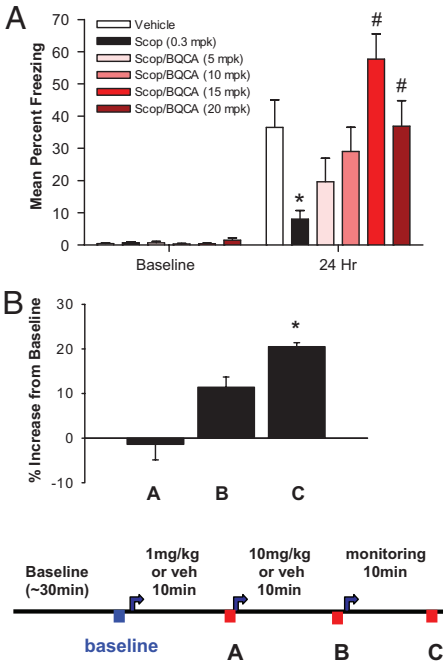

Fig. 4. Physiological effects of BQCA. (*A*) Contextual fear conditioning. On day one animals received 0.3 mg/kg scopolamine ± BQCA administered IP at the indicated doses before being introduced to a novel environment and receiving two foot shocks. Twenty-four hours later animals (n = 12–16/group) were reintroduced to the environment and freezing measured by automated detection equipment. Shown is mean percent of time freezing (± SEM.). Data are representative of four experiments. *, Different from vehicle; #, different from scopolamine + vehicle ($P < 0.05$, Dunnet test). (*B*) Increased cerebral blood flow in anesthetized rats in response to BQCA. Data were averaged over 1 min at the indicated time points (*A–C*) and is expressed as mean percent change from baseline ± SEM. (n = 4 animals). *, Significantly different from baseline, $P < 0.01$, repeated measures ANOVA, t test.

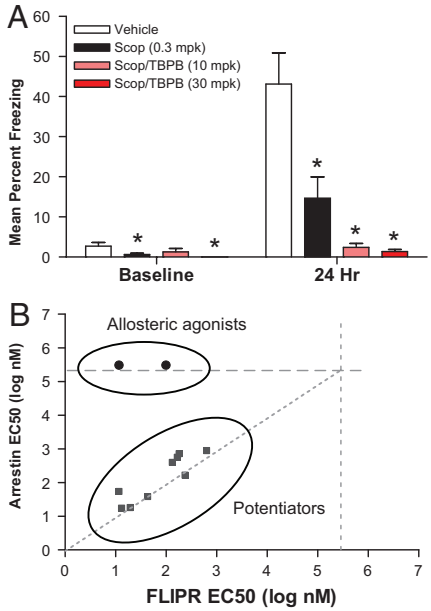

Fig. 5. Allosteric agonists do not reverse scopolamine deficits in contextual fear conditioning or recruit β-arrestin. (*A*) Effects of TBPB at 10 and 30 mg/kg (mpk) in contextual fear conditioning. Shown is mean (n = 16/group) percent of time exhibiting freezing behavior + SEM *, Different from vehicle alone ($P < 0.05$, Dunnet test). Experiment was repeated twice with similar results. (*B*) TBPB and AC-42 (allosteric agonists, top circle) do not significantly recruit β-arrestin to hM_1 compared to BQCA and 8 related allosteric potentiators (allosteric potentiators, bottom circle). Potencies (IP) for these compounds in calcium mobilization as measured by FLIPR (x axis) were compared to β-arrestin recruitment as measured by enzyme complementation (y axis). In both experiments, CHO cells stably expressing hM_1 were used, for β-arrestin hM_1 is fused to a portion of β-galactosidase while a complementary β-galactosidase fragment is fused to β-arrestin. Thus β-galactosidase activity is an indirect measure of β-arrestin recruitment. Values along the dashed lines indicate that no inflection point in the slope was observed at the highest concentrations tested (representative dose–response curves are in Fig. S8*C*). Note that the allosteric potentiators show a correlation between calcium mobilization and β-arrestin recruitment whereas for the allosteric agonists IP values were only measurable in calcium mobilization.

Contextual Fear Conditioning. To examine the role of M_1 in memory we measured contextual fear conditioning (CFC) in mice. This task requires the hippocampus (18) where M_1 is highly expressed. Subjects were introduced to a novel environment where they received an aversive stimulus (foot shock). The next day the animal exhibited freezing behavior, indicative of fear, if it associated the aversive stimulus with the environment. Scopolamine, a nonselective muscarinic antagonist, was dosed 30 min before introduction to the novel environment to block formation of this association (19) (Fig. 4*A*). BQCA was co-dosed at 5, 10, 15, and 20 mg/kg i.p. (IP) with scopolamine on training day and had no effect on freezing behavior at that time. When animals were reintroduced into the test chamber those given scopolamine previously showed marked reduction in freezing compared to controls. However animals that had been co-dosed with BQCA at 15 or 20 mg/kg had no scopolamine deficit ($P < 0.05$, ANOVA, Dunnett test). This experiment was repeated with structurally distinct derivatives of BQCA that are also >100-fold selective for M_1 with similar results. Thus BQCA prevents scopolamine-induced memory deficits in CFC.

Cerebral Blood Flow. ACh promotes cerebral blood flow (CBF) (20) and M_1 is expressed in cortical neurons and endothelial cells (21), however a role for M_1 in CBF has not been defined. BQCA, but not vehicle, intravenously infused into anesthetized rats at 10 mg/kg caused a sustained increase in CBF by 20.5 ± 0.9% as measured by laser Doppler flowmetry ($F_{(2, 207)} = 14.1$; $P = 0.005$) (Fig. 4*B*). BQCA had no effect on arterial pressure ($F_{(2, 243)} = 0.51$; $P = 0.63$) and caused a brief but significant 11.0 ± 2.1% increase in heart rate ($F_{(2, 70)} = 6.1$; $P = 0.036$). Thus BQCA promotes CBF in rats.

Effects on Sleep. The cholinergic system modulates wakefulness and the onset of REM sleep (22, 23). To assess the role of M_1 in sleep, rats were dosed with BQCA at 10 mpk IP 30 min before the beginning of the light (inactive) cycle for seven days. Electrocorticogram and electromyogram activities were recorded and the time spent in active wake, light sleep, REM, and delta sleep were averaged in 30 min epochs across 7 days of testing. Over the first 90 min of the light phase BQCA increased the time spent in active wake and light sleep while concomitantly decreasing delta sleep ($P < 0.001$, Student's t test) (Fig. S6). By 120-min sleep patterns between BQCA-treated and control animals were similar and no lasting effects where observed.

Allosteric Agonists Exhibit Differential Efficacy. We then compared the activities of BQCA to TBPB, an M_1-selective allosteric agonist that has anti-psychotic-like activity in rats (14). Like TBPB, BQCA at 10 and 30 mg/kg IP repressed amphetamine-induced locomotion in mice (Fig. S7*A*). However TBPB did not reverse the scopolamine deficit in CFC at 10 or 30 mg/kg IP (Fig. 5*A*); and similarly the allosteric agonist AC-42 was without effect at 3, 10, and 30 mg/kg (12) (Fig. S7*B*). To explore this difference we measured recruitment of β-arrestin, which mediates GPCR internalization and second messenger signaling (24). CHO cells expressing hM_1 fused to a portion of β-galactosidase and β-arrestin fused to a complementary fragment of β-galactosidase (25) were treated with TBPB, AC-42, or ACh ± BQCA or eight BQCA analogs. Recruitment of

PHARMACOLOGY

the β-galactosidase/β-arrestin fusion protein to M_1 restores β-galactoside activity. BQCA and its analogs potentiated ACh-induced β-arrestin recruitment with EC_{50} values correlated with potency in calcium mobilization (Fig. 5*B*). Neither TBPB nor AC-42 induced β-arrestin recruitment beyond ≈20% of maximal activity up to 10 μM, thus no EC_{50} was measurable (Fig. 5*B* and Fig. S7*C*). Together these data indicate that BQCA diverges mechanistically from these allosteric agonists.

Discussion

Despite the therapeutic potential of M_1, high selectivity against other mAChRs has not been achieved. Here we describe BQCA, which sensitizes M_1 to ACh up to 100-fold (Fig. 1). It has little effect on M_2-M_5 or other class A GPCRs (Fig. 2 and Fig. S3), or in >300 other assays. In the absence of M_1 BQCA does not enhance ACh-mediated inositol phosphate metabolism or induce c-fos or arc RNA or ERK phosphorylation in the brain (Fig. 2 and Fig. S4). BQCA does not interact with the ACh site but instead enhances ACh activity from an allosteric pocket (Fig. 3). Molecular modeling combined with site-directed mutagenesis identified a potential extracellular interaction site conserved in M_1 that diverges in other mAChRs (Fig. 3). Interestingly Y179, one of the residues required for BQCA activity, corresponds to Y177 in M_2, which is in a common site critical for multiple allosteric agonists (26). Thus probing this region further could improve our understanding of allosteric modulation.

We used BQCA to explore the function of M_1 in brain function. BQCA promotes the learned association of a novel environment with an aversive stimulus, a task dependent on the hippocampus and sensitive to the anti-muscarinic scopolamine (Fig. 4). Selectively sensitizing M_1 with BQCA fully overcomes the amnestic effects of scopolamine in this model. These results contrast with data in $M_1^{-/-}$ mice (27) and with an M_1 selective antagonist, VU0255035 (28). In the former study the $M_1^{-/-}$ mice showed no deficit in CFC, and in the latter study VU0255035 reduced pilocarpine-induced seizures in rats, which requires M_1 (29), but did not interfere with CFC. Together these data suggest that deletion or inhibition of M_1 does not interfere with this form of memory. However our data indicate that M_1 activation during acquisition promotes memory, perhaps indicating that M_1 is not required for memory formation in CFC, but rather reinforces it by stimulating other receptor signaling systems such as the NMDA receptor (6). Based on prior work (30) M_1 expressed in CA3 hippocampal neurons may be specifically involved in this positive modulation of memory.

We found that BQCA enhanced CBF (Fig. 4), a function of ACh attributed to M_5 based on receptor localization and knockout mouse experiments (31, 32). Our data indicate that M_1 also regulates CBF perhaps via neurovascular coupling. The cholinergic system also modulates sleep; ACh levels are elevated in the cortex and hippocampus during wakefulness and REM sleep relative to slow wave delta sleep (33). When dosed before the onset of sleep BQCA increased wakefulness and inhibited delta sleep without significant lasting effects (Fig. S7). This observation is consistent with M_1 promoting arousal and suggests that ACh levels decline during slow wave sleep in part to reduce M_1 activity.

Since allosteric ligands of GPCRs can selectively modulate some, but not all, available second messenger signaling systems (34) we compared BQCA to the allosteric agonists TBPB and AC-42. Both BQCA and TBPB inhibit amphetamine-induced locomotion in mice (14 and Fig. S7), suggesting that they modulate striatal dopaminergic activity. In contrast neither TBPB nor AC-42 reversed scopolamine deficits in CFC (Fig. 5 and Fig. S7). A potential reason for this difference is that these compounds do not efficiently induce β-arrestin recruitment as measured by enzyme complementation (Fig. 5). Other studies show that AC-42 does not activate all G-proteins coupled to M_1 (35), together suggesting that these allosteric agonists may exhibit ligand bias (36), the propensity to activate a subset of signaling pathways presumably by stabilizing unique receptor conformations. Since β-arrestins couple M_1 to diacyl glycerol kinases (24) and likely play other signaling functions, it will be interesting to identify β-arrestin-dependent responses triggered by ACh in hippocampal neurons.

In summary we identified a highly selective positive allosteric modulator of the M_1 muscarinic receptor. This compound will allow for further understanding of allosterism at GPCRs, insight into the function of M_1, and potentially a class of therapies for diseases involving impaired function of the central cholinergic system.

Materials and Methods

Materials. Reagents were from Sigma unless noted, and animals were from Taconic Farms. Procedures were approved by the Institutional Animal Care and Use committee (IACUC) in accordance with the National Institutes of Health *Guide for the Care and Use of Laboratory Animals*. *Chrm1*$^{-/-}$ animals were provided by Dr. Neil Nathanson (37).

Data Presentation. Experimental values are the mean of *n* independent determinations ± SEM. unless otherwise indicated.

High-Throughput Screening. Using an automated screen for Gq activation by GPCRs (38), 2×10^3 cells/well of CHO cells expressing human M_1 and an NFAT-responsive β-lactamase reporter were plated into 3,456 well plates and treated with 15 nM ACh plus 6.23 μM of test compound for 4 h before adding CCF4-AM (Invitrogen), to detect β-lacatamase activity.

Fluorometric Imaging Plate Reader (FLIPR). CHO-NFAT cells expressing human mAChRs or rhesus, dog, mouse, or rat M_1 (in CHO-K1, ATCC) were plated (25,000 cells/well) in clear-bottomed polyd-lysine (PDL)-coated 384-well plates in growth medium using Labsystems Multidrop. Receptor expression levels for the human lines were measured by radioligand binding and were M_1 (0.70 ± 0.03), M_2 (3.22 ± 0.08), M_3 (0.53 ± 0.04), M_4 (1.61 ± 0.09), and M_5 (0.80 ± 0.07) pmol/mg protein (n = 3). Cells were grown overnight 37 °C/6% CO_2, washed 3 × 100 μL assay buffer (Hanks' balanced salt solution/20 mM HEPES/2.5 mM probenecid/0.1% BSA) then incubated with 1 μM Fluo-4 a.m. (Invitrogen) 1 h at 37 °C/6% CO_2. Extracellular dye was removed and Ca^{2+} was measured with a $FLIPR_{384}$ fluorometric imaging plate reader (Molecular Devices) during incubation with compound 4 min followed by 4 min with the EC_{15} of ACh.

IP1. Cortical/hippocampal neurons from embryonic day 15–16 wild-type or *Chrm1* $(M_1)^{-/-}$ mice were plated (70,000 cells/well) in PDL 96-well white plates and maintained 9 days. IP1 levels were meausured using HTRF (Cisbio Bioassays) using Envision (Perkin-Elmer) following 10-min incubation with BQCA then 30 min with ACh. Ten mM LiCl was added to block degradation of inositol phosphates.

β-Arrestin. The hM_1AchR PathHunter CHO cells (DiscoveRx) stably expressing two fragments of β-galactosidase, one fused to M_1 and the other to β-arrestin, were treated with ligand and β-galactosidase complementation was monitored by PathHunter Detection reagent and read on a ViewLux (Perkin-Elmer). Compounds were assayed in 384-well plates ± ACh EC_{15}.

Binding Assays. Competition binding reactions used 25 μg human M_1 CHO membrane protein (Perkin-Elmer), test compounds or vehicle, and 0.15 nM [^{3}H]NMS in 96-well deep-well plates. Binding reactions (30 °C for 2–3 h) were terminated by rapid filtration. Nonspecific binding was determined by adding 10 μM atropine. Filter plates were washed 4× with ice-cold 20 mM HEPES, 100 mM NaCl, and 5 mM $MgCl_2$, pH 7.4 using a 96-well Perkin-Elmer harvester. Plates were dried and radioactivity counted with a TopCount NXT microplate scintillation counter (Perkin-Elmer). Counts were normalized to maximal specific binding with vehicle. The GTPγS assay reactions used 25 μg CHO membrane protein, 2 μM GDP, and 0.1 nM [^{35}S]GTPγS in a total volume of 500 μL; samples were incubated in a 96-well deep-well plate (0.5 h at 30 °C). The binding assay buffer, reaction termination, and counting were as above.

Counterscreens. BQCA was tested in duplicate (10 μM) for activity or radioligand displacement on >300 enzymes and receptors using commercially available assays (MDS Pharma). For potentiation of class A GPCRs, BQCA (37.5 μM) was analyzed ± agonist by FLIPR in CHO cells stably expressing the receptors using GPCRprofiler, details are available from the manufacturer (Millipore).

Molecular Modeling. Mutations were made by site-directed mutagenesis and sequence confirmed before transient transfection into CHO cells. Maximal bind-

ing activity for [3H]-NMS was measured in membrane preparations from wild-type, Y179A, and W400A and was 1.90 ± 0.2, 2.70 ± 0.44, 1.50 ± 0.46 pmol/mg ($n = 3$). The M_1 model was built from rhodopsin (39, 40); see *SI Text*.

Immediate Early Gene Induction. Wild-type or *Chrm1* (M_1) $^{-/-}$ mice were individually housed and desensitized by handling 5 separate times before the experiment. Mice ($n = 5$/group) received 15 mg/kg BQCA in 5% betacyclodextrin/saline IP. After 1.5 h animals were euthanized; in situ hybridization has been described in detail (41).

ERK Phosphorylation. Adult (4–6 week) male mice ($n = 6$) were dosed with 15 mg/kg PO BQCA in sterile water or with vehicle alone and 1 h later cortical and hippocampal samples were collected. Homogenization was performed on ice in 0.32 M sucrose/1 mM HEPES/1 mM $MgCl_2$/1 mM EDTA/1 mM $NaHCO_3$ (pH 7.4) supplemented with protease and phosphatase inhibitors. Thirty μg total protein was resolved on 10% SDS gels and probed with rabbit polyclonal anti-p44/42 MAPK (T202/Y204) or mouse monoclonal anti-p42 MAP Kinase (3A7) (Cell Signal Technologies). Immunoblots were quantitated on a Li-Cor Odyssey infrared imager (Li-Cor Biosciences).

Contextual Fear Conditioning. On day one 10-week-old experimentally naïve male B6SJL mice ($n = 12$–16/group) were dosed IP with BQCA in 5% betacyclodextrin and/or 0.3 mg/kg scopolamine in 0.9% saline 30 min before placement into a chamber (MED-VFC-M, Med Associates) for 2 min before 2 tone-footshock pairings (3 kHz, 85 dB tone for 30 s co-terminated with a 0.5 mA, 1 s shock) 2 min apart. Mice were removed to their home cage 30 s after the last pairing. Twenty-four hours later mice were placed into the same chamber and freezing was measured by Video Freeze (Med Associates).

Cerebral Blood Flow. Six- to eight-week-old male Sprague-Dawley rats were anesthetized with urethane (1 g/kg IP). Depth of anesthesia was monitored by toe pinch; supplemental urethane (10% of initial dose) was given to achieve deep anesthesia. Body temperature was kept at 37 °C via a heating pad and rectal temperature feedback probe. A femoral artery was cannulated with PE50 tubing to record arterial pressure and heart rate via a pressure transducer (ADInstruments); the femoral vein was cannulated for drug infusion (20 μL/min). Animals were placed in a stereotactic frame and a midline incision exposed the skull. A burr hole was drilled over the frontal cortex (1.0 mm anterior and 4.0 mm lateral to bregma) leaving the dura intact. A laser Doppler probe connected to a data acquisition system (PowerLab 8/30, ADInstruments) was placed over the hole. CBF recordings began after MAP, HR and CBF were stable for 15–20 min. Data are presented as percent increase over resting CBF.

Sleep Electroencephalography (EEG). Sleep was evaluated in adult male Sprague-Dawley rats (age 3–8 months) chronically implanted with telemetric physiological monitors recording electrocorticogram and electromyogram activities as described (42). Dosing was 30 min before lights on for 7 days in a crossover experiment.

Amphetamine-Induced Locomotor Activity. Six week old male B6SJL mice ($n = 12$) were dosed IP with the indicated dose of BQCA and placed into standard open field box equipped with infrared motion sensors for 20 min. They were then given 2.5 mg/kg amphetamine then returned to the open field box and tracked for 40 additional minutes.

ACKNOWLEDGMENTS. We thank Dr. Neil Nathanson, University of Washington, for providing the $M_1^{-/-}$ mice. We thank the following for technical support and scientific input: Robert Breese, Michele Crouthamel, Pierre Mallorga, Christine Ng, Kenji Ohwaki, Jonathan Schneeweis, Mark Bilodeau, Samuel Graham, George Hartman, Kenneth Koblan, Kenneth Koeplinger, John Renger, Sethu Sankaranarayanan, Adam Simon, Charles Thompson, and Joseph Vacca.

1. Geula C (1998) Abnormalities of neural circuitry in Alzheimer's disease: Hippocampus and cortical cholinergic innervation. *Neurology* 51:S18–29.
2. Hansen R, et al. (2008) Efficacy and safety of donepezil, galantamine, and rivastigmine for the treatment of Alzheimer's disease: A systematic review and meta-analysis. *Clin Interv Aging* 3:211–225.
3. Levey A (1996) Muscarinic acetylcholine receptor expression in memory circuits: Implications for treatment of Alzheimer disease. *Proc Natl Acad Sci USA* 93:13541–13546.
4. Lanzafame A, Christopoulos A, Mitchelson F (2003) Cellular signaling mechanisms for muscarinic acetylcholine receptors. *Receptors Channels* 9:241–260.
5. Felder C (1995) Muscarinic acetylcholine receptors: Signal transduction through multiple effectors. *FASEB J* 9:619–625.
6. Marino M, Rouse S, Levey A, Potter L, Conn J (1998) Activation of the genetically defined m1 muscarinic receptor potentiates N-methyl-D-aspartate (NMDA) receptor currents in hippocampal pyramidal cells. *Proc Natl Acad Sci USA* 95:11465–11470.
7. Jones S (1993) Muscarinic receptor subtypes: Modulation of ion channels. *Life Sci* 52:457–464.
8. Nadler L, et al. (1999) Molecular analysis of the regulation of muscarinic receptor expression and function. *Life Sci* 64:375–379.
9. Liu L, et al. (2006) M1 muscarinic receptors inhibit L-type Ca2+ current and M-current by divergent signal transduction cascades. *J Neurosci* 26:11588–11598.
10. Bodick N, et al. (1997) Effects of xanomeline, a selective muscarinic receptor agonist, on cognitive function and behavioral symptoms in Alzheimer disease. *Arch Neurol* 54:465–473.
11. Fisher A (2008) Cholinergic treatments with emphasis on m1 muscarinic agonists as potential disease-modifying agents for Alzheimer's disease. *Neurotherapeutics* 5:433–442.
12. Spalding T, et al. (2002) Discovery of an ectopic activation site on the M(1) muscarinic receptor. *Mol Pharmacol* 61:1297–1302.
13. Birdsall N, Lazareno S (2005) Allosterism at muscarinic receptors: Ligands and mechanisms. *Mini Rev Med Chem* 5:523–543.
14. Jones C, et al. (2008) Novel selective allosteric activator of the M1 muscarinic acetylcholine receptor regulates amyloid processing and produces antipsychotic-like activity in rats. *J Neurosci* 28:10422–10433.
15. Marlo J, et al. (2009) Discovery and characterization of novel allosteric potentiators of M1 muscarinic receptors reveals multiple modes of activity. *Mol Pharmacol* 75:577–588.
16. Conklin B, Farfel Z, Lustig K, Julius D, Bourne H (1993) Substitution of three amino acids switches receptor specificity of Gq alpha to that of Gi alpha. *Nature* 363:274–276.
17. Thomas G, Huganir R (2004) MAPK cascade signaling and synaptic plasticity. *Nat Rev Neurosci* 5:173–183.
18. Kim J, Fanselow M (1992) Modality-specific retrograde amnesia of fear. *Science* 256:675–677.
19. Young S, Bohenek D, Fanselow M (1995) Scopolamine impairs acquisition and facilitates consolidation of fear conditioning: differential effects for tone vs context conditioning. *Neurobiol Learn Mem* 63:174–180.
20. Sato A, Sato Y, Uchida S (2004) Activation of the intracerebral cholinergic nerve fibers originating in the basal forebrain increases regional cerebral blood flow in the rat's cortex and hippocampus. *Neurosci Lett* 361:90–93.
21. Elhusseiny A, Cohen Z, Olivier A, Stanimirovic D, Hamel E (1999) Functional acetylcholine muscarinic receptor subtypes in human brain microcirculation: Identification and cellular localization. *J Cereb Blood Flow Metab* 19:794–802.
22. Hobson J, Datta S, Calvo J, Quattrochi J (1993) Acetylcholine as a brain state modulator: triggering and long-term regulation of REM sleep. *Prog Brain Res* 98:389–404.
23. Perry E, Walker M, Grace J, Perry R (1999) Acetylcholine in mind: A neurotransmitter correlate of consciousness? *Trends Neurosci* 22:273–280.
24. Nelson C, et al. (2007) Targeting of diacylglycerol degradation to M1 muscarinic receptors by beta-arrestins. *Science* 315:663–666.
25. Yan X, et al. (2002) Cell-based high-throughput screening assay system for monitoring G protein-coupled receptor activation using beta-galactosidase enzyme complementation technology. *J Biomol Screen* 7:451–459.
26. May L, et al. (2007) Structure-function studies of allosteric agonism at M2 muscarinic acetylcholine receptors. *Mol Pharmacol* 72:463–476.
27. Miyakawa T, Yamada M, Duttaroy A, Wess J (2001) Hyperactivity and intact hippocampus-dependent learning in mice lacking the M1 muscarinic acetylcholine receptor. *J Neurosci* 21:5239–5250.
28. Sheffler D, et al. (2009) A novel selective muscarinic acetylcholine receptor subtype 1 (M1 mAChR) antagonist reduces seizures without impairing hippocampal-dependent learning. *Mol Pharmacol* 2009.
29. Bymaster F, et al. (2003) Role of specific muscarinic receptor subtypes in cholinergic parasympathomimetic responses, in vivo phosphoinositide hydrolysis, and pilocarpine-induced seizure activity. *Eur J Neurosci* 17:1403–1410.
30. Rogers J, Kesner R (2004) Cholinergic modulation of the hippocampus during encoding and retrieval of tone/shock-induced fear conditioning. *Learn Mem* 11:102–107.
31. Yamada M, et al. (2001) Cholinergic dilation of cerebral blood vessels is abolished in M(5) muscarinic acetylcholine receptor knockout mice. *Proc Natl Acad Sci USA* 98:14096–14101.
32. Phillips J, Vidovic M, Hill C (1997) Variation in mRNA expression of alpha-adrenergic, neurokinin and muscarinic receptors amongst four arteries of the rat. *J Auton Nerv Syst* 62:85–93.
33. Marrosu F, et al. (1995) Microdialysis measurement of cortical and hippocampal acetylcholine release during sleep-wake cycle in freely moving cats. *Brain Res* 671:329–332.
34. Leach K, Sexton P, Christopoulos A (2007) Allosteric GPCR modulators: Taking advantage of permissive receptor pharmacology. *Trends Pharmacol Sci* 28:382–389.
35. Thomas R, Mistry R, Langmead C, Wood M, Challiss R (2008) G protein coupling and signaling pathway activation by m1 muscarinic acetylcholine receptor orthosteric and allosteric agonists. *J Pharmacol Exp Ther* 327:365–374.
36. Shukla A, et al. (2008) Distinct conformational changes in beta-arrestin report biased agonism at seven-transmembrane receptors. *Proc Natl Acad Sci USA* 105:9988–9993.
37. Hamilton S, et al. (1997) Disruption of the m1 receptor gene ablates muscarinic receptor-dependent M current regulation and seizure activity in mice. *Proc Natl Acad Sci USA* 94:13311–13316.
38. Kunapuli P, et al. (2003) Development of an intact cell reporter gene beta-lactamase assay for G protein-coupled receptors for high-throughput screening. *Anal Biochem* 314:16–29.
39. Palczewski K, et al. (2000) Crystal structure of rhodopsin: A G protein-coupled receptor. *Science* 289:739–745.
40. Fredriksson R, Lagerstrom M, Lundin L, Schioth H (2003) The G-protein-coupled receptors in the human genome form five main families. Phylogenetic analysis, paralogon groups, and fingerprints. *Mol Pharmacol* 63:1256–1272.
41. Austin C, Ky B, Ma L, Morris J, Shughrue P (2004) Expression of Disrupted-In-Schizophrenia-1, a schizophrenia-associated gene, is prominent in the mouse hippocampus throughout brain development. *Neuroscience* 124:3–10.
42. Renger J, Dunn S, Motzel S, Johnson C, Koblan K (2004) Sub-chronic administration of zolpidem affects modifications to rat sleep architecture. *Brain Res* 1010:45–54.